JOURNAL OF MATERIALS SCIENCE **39** (2004) 133–139

Compositional effects on densification and microstructural evolution of bismuth titanate

J. S. PATWARDHAN, M. N. RAHAMAN
University of Missouri-Rolla, Department of Ceramic Engineering, Rolla, Missouri 65409, USA
E-mail: rahaman@umr.edu

The effects of small compositional variations on the densification and microstructural evolution of bismuth titanate ($Bi_4Ti_3O_{12}$) powder compacts were investigated during sintering and during hot forging. For a nominally stoichiometric $Bi_4Ti_3O_{12}$ composition, sintering commenced at ~870°C, leading to a relatively dense microstructure (relative density >97% of the theoretical value) with randomly aligned elongated grains after 1 h at 1100°C. Small additions (1 weight percent) of Bi_2O_3 or TiO_2 to the nominally stoichiometric $Bi_4Ti_3O_{12}$ composition shifted the onset of sintering to lower or higher temperatures, respectively, but did not significantly alter the final density. Hot forging produced a microstructure of aligned, elongated grains. The small compositional variations did not seriously influence the ability to develop the elongated grain alignment. However, subsequent annealing of the hot forged materials produced significant changes in the aligned grain microstructure. The elongated grain alignment in the nominally stoichiometric $Bi_4Ti_3O_{12}$ composition was destroyed during subsequent annealing for less than 2 h at 1100°C.

1. Introduction

Commonly, ceramic microstructures consist of randomly oriented, equiaxial grains that give rise to isotropic engineering properties normally required for most technological applications. The development of a textured microstructure consisting of aligned, elongated grains can provide unique anisotropic properties for enhancing the usefulness of certain ceramics, such as piezoelectric ceramics for sensing and actuating devices. The basic requirements for developing a microstructure of elongated, aligned grains during the fabrication of granular materials are anisotropic grain growth and alignment of the anisometric (elongated) grains. Anisotropic grain growth is frequently observed in materials with the hexagonal crystal structure such as Al_2O_3 [1, 2], chainlike structures such as mullite [3, 4], and layered structures such as $Bi_4Ti_3O_{12}$ [5]. The mechanism of growth is not clear but several factors have been suggested as being important for the process. These include anisotropic surface energies, twinning, segregation of impurities and dopants, and anisotropic wetting by liquid phases [2, 6]. Several processing techniques have been employed to develop grain alignment in ferroelectric ceramics, including hot forging [7, 8], hot pressing [9, 10], tape casting [11, 12], and templated grain growth [13, 14].

Bismuth titanate ($Bi_4Ti_3O_{12}$) is a candidate material for high temperature piezoelectric applications, memory storage, and optical displays because of its high Curie temperature (~675°C) and electrooptical properties [15–18]. Textured $Bi_4Ti_3O_{12}$ have been achieved in several studies [8–14]. However, the mechanism of grain alignment during hot forging or hot pressing is not clear. Furthermore, the effect of deviations from the stoichiometric $Bi_4Ti_3O_{12}$ composition on texture development has received little attention. The stability of the textured microstructure to subsequent heat treatment is also unclear.

According to published phase diagram data of Speranskaya *et al.* [19], three incongruently-melting compounds exist in the Bi_2O_3-TiO_2 system (Fig. 1): $Bi_4Ti_3O_{12}$ (peritectic melting temperature ≈1210°C), the bismuth-rich phase Bi_8TiO_{14} (peritectic melting temperature ≈865°C) and the titanium-rich $Bi_2Ti_4O_{11}$ (peritectic melting temperature ≈1275°C). The data of Bruton [20] are similar to those given by Speranskaya *et al.*, except that the bismuth-rich compound is $Bi_{12}TiO_{20}$, melting incongruently at ~873°C. The bismuth-rich compound has also been identified as $Bi_{12}TiO_{20}$ by Levin and Roth [21] who suggested that it is congruently melting, and by Morrison [22] who concluded that congruent melting is favored but that the departure from congruent melting is small. Morrison also found a higher peritectic melting temperature (~920°C) than those obtained by Speranskaya *et al.* [19] and Bruton [20]. It is clear from the phase diagram data that for the fabrication temperatures commonly used for $Bi_4Ti_3O_{12}$ (1000 to 1150°C), small deviations from the stoichiometric $Bi_4Ti_3O_{12}$ composition will lead to solid state sintering (for TiO_2-rich compositions) or sintering in the presence of a liquid phase (for Bi_2O_3-rich compositions). The influence of such

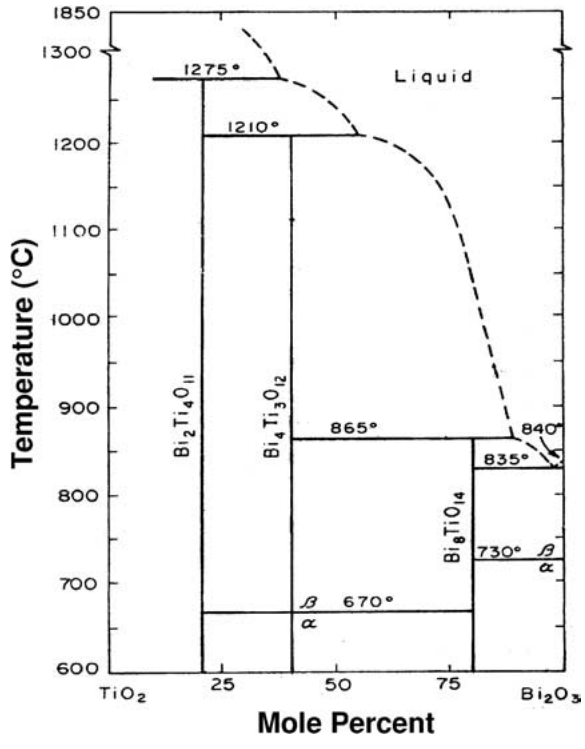

Figure 1 Phase diagram for the system Bi_2O_3-TiO_2 (after [19]).

compositional variations on the texture development of $Bi_4Ti_3O_{12}$ has not been investigated systematically.

The objective of the present study was to investigate how small compositional variations (excess of Bi_2O_3 or TiO_2) influence microstructure evolution of $Bi_4Ti_3O_{12}$ during sintering and during hot forging. The stability of the hot-forged, textured microstructure to subsequent annealing was also investigated.

2. Experimental procedure

A conventional process involving the calcination of mixed oxides was used to prepare the $Bi_4Ti_3O_{12}$ powder. Starting powders of Bi_2O_3 powder (Ferro Corp., Pen Yan, NY; average particle size $\approx$4 μm; purity $\approx$99.9%) and TiO_2 powder (Ferro Corp., Pen Yan, NY; average particle size $\approx$3 μm; purity $\approx$99.9%), were weighed out in the molar ratio of 2:3 and mixed by ball milling for 24 h in a polyethylene container while dispersed in isopropanol, using high purity zirconia balls as the milling media. The mixture was stirred in a beaker until it was nearly dry, heated at 100°C in an oven to evaporate the remaining liquid and ground lightly in an agate mortar and pestle. The powder was calcined in a high purity Al_2O_3 crucible for 1 h at 600°C followed by 4 h at 850°C to produce $Bi_4Ti_3O_{12}$. After calcination, the powder was again ball-milled (under the conditions described earlier) to break down agglomerates, dried, lightly ground in an agate mortar and pestle and sieved using a 100-mesh nylon screen (nominal aperture = 150 μm). The composition of powders prepared from a Bi_2O_3:TiO_2 molar ratio of 2:3 will be referred to as nominal $Bi_4Ti_3O_{12}$. Powders with 1 weight percent (wt%) excess TiO_2 (referred to as TiO_2-rich $Bi_4Ti_3O_{12}$) or 1 wt% excess Bi_2O_3 (Bi_2O_3-rich $Bi_4Ti_3O_{12}$) were also prepared using the same procedure.

The powders were pressed in a uniaxial die at $\sim$35 MPa and then cold isostatically pressed at $\sim$275 MPa to produce cylindrical compacts ($\sim$6 mm in diameter by 5 mm high). The green densities of the compacts, determined from their mass and dimensions, were 60–65% of the theoretical density of $Bi_4Ti_3O_{12}$ (equal to 8.04 g/cm^3 according to [23]). The powder compacts were sintered in air in a dilatometer (1600 C; Theta Industries Inc., Port Washington, NY) that allowed continuous monitoring of the shrinkage kinetics. Sintering was performed for 1 h at 1100°C using a heating rate of 5°C/min and a cooling rate of 10°C/min. The densities of the sintered samples were determined from the green density ρ_0 and the shrinkage $\Delta L/L_0$ using the equation:

$$\rho = \frac{\rho_0}{(1 - \Delta L/L_0)^3} \tag{1}$$

where L_0 is the initial length of the compact, and $\Delta L = L_0 - L$, where L is the instantaneous length of the compact. For comparison, the final densities of the sintered samples were measured using the Archimedes method.

Hot forging of cylindrical powder compacts (12.5 mm in diameter by 9 mm in height) was performed in air under a load of 5 MPa at isothermal temperatures of 950°C and 1050°C in an Instron testing machine fitted with a programmable furnace. (The heating and cooling rates were 10°C/min.) The axial shrinkage during hot forging was monitored using a linear voltage displacement transducer (LVDT). Prior to hot forging, the compacts were fired at 5°C/min to fixed temperatures to produce samples with relative densities in the range of 70–90% in order to investigate the effect of starting density on grain alignment during hot forging. The densities of the hot forged samples were measured by the Archimedes method. Specimens were sectioned from the hot forged materials and annealed in air at temperatures of 1000–1100°C to observe the evolution of the textured microstructure.

X-ray diffraction (XDS 2000; Scintag Inc., Sunnyvale, CA) was used to identify the crystalline phases in the samples. For the hot forged materials, the degree of texturing was determined from the X-ray diffraction (XRD) patterns by the Lotgering method [24]. The samples were scanned at 0.03 degrees/min from 10 to 60° 2θ on the surfaces perpendicular and parallel to the applied pressure. The degree of orientation, referred to as the Lotgering factor f was determined from the relation:

$$f = \frac{P - P_0}{1 - P_0} \tag{2}$$

where $P = \Sigma I(00l)/\Sigma I\ (hkl)$, where $\Sigma I(00l)$ and $\Sigma I\ (hkl)$ are the sums of the intensities of $(00l)$ and (hkl) reflections, respectively, between 10° and 60° 2θ, and P_0 is the value of P for a randomized powder sample, taken in this study as the calcined powder.

Scanning electron microscopy (JEOL T330A) was used to observe the microstructure of the fabricated materials. Samples for scanning electron microscopy (SEM) were prepared by polishing down to 0.1 μm diamond finish, followed by thermal etching for 1 h at 950°C.

3. Results and discussion

Fig. 2 shows the data for the relative density as function of temperature during constant heating rate sintering at 5°C/min to 1100°C for powder compacts with the nominal $Bi_4Ti_3O_{12}$ composition, Bi_2O_3-rich $Bi_4Ti_3O_{12}$, and TiO_2-rich $Bi_4Ti_3O_{12}$. Whereas the sintering curves have approximately the same shape and with approximately the same final density (~97% of the theoretical), small compositional variation has a significant effect on the temperature range of sintering. When compared to nominal $Bi_4Ti_3O_{12}$ that starts to show measurable densification at ~875°C, excess Bi_2O_3 lowers the sintering temperature while excess TiO_2 raises the sintering temperature. The onset of sintering for the nominally stoichiometric $Bi_4Ti_3O_{12}$ composition corresponds to ~0.75 of the peritectic melting temperature (≈1210°C). While the presence of a small concentration of liquid phase cannot be ruled out, solid-state sintering can provide a valid mechanism for sintering at temperatures greater than ~0.5–0.6 of the peritectic melting temperature.

Bi_2O_3-rich $Bi_4Ti_3O_{12}$ starts to show measurable shrinkage at temperatures as low as ~800°C. The phase diagram (Fig. 1) indicates that a liquid phase in Bi_2O_3-rich $Bi_4Ti_3O_{12}$ compositions is formed at 865–870°C (corresponding to the peritectic melting temperature for the Bi_8TiO_{14} or $Bi_{12}TiO_{20}$ phase). This lowering of the onset of sintering to temperatures below the liquid formation temperature is not clear in this case. However, enhanced densification at temperatures of up to a few hundred degrees Celsius below the liquid formation temperature has also been observed in several ceramic systems, including the well-studied ZnO-Bi_2O_3 system [25, 26]. The raising of the sintering temperature for the case of the TiO_2-rich composition is also not clear but a possible factor may be the presence of a dispersion of fine second phase particles (presumably with the composition of $Bi_2Ti_4O_{11}$) which reduce matter transport along the grain boundaries.

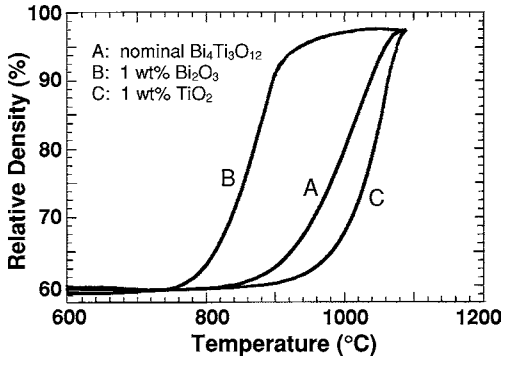

Figure 2 Relative density versus temperature for powder compacts with a nominal $Bi_4Ti_3O_{12}$ composition, a Bi_2O_3-rich $Bi_4Ti_3O_{12}$ composition (1 wt% excess Bi_2O_3), and a TiO_2-rich $Bi_4Ti_3O_{12}$ composition (1 wt% excess TiO_2), during constant heating rate sintering (5°C/min to 1100°C).

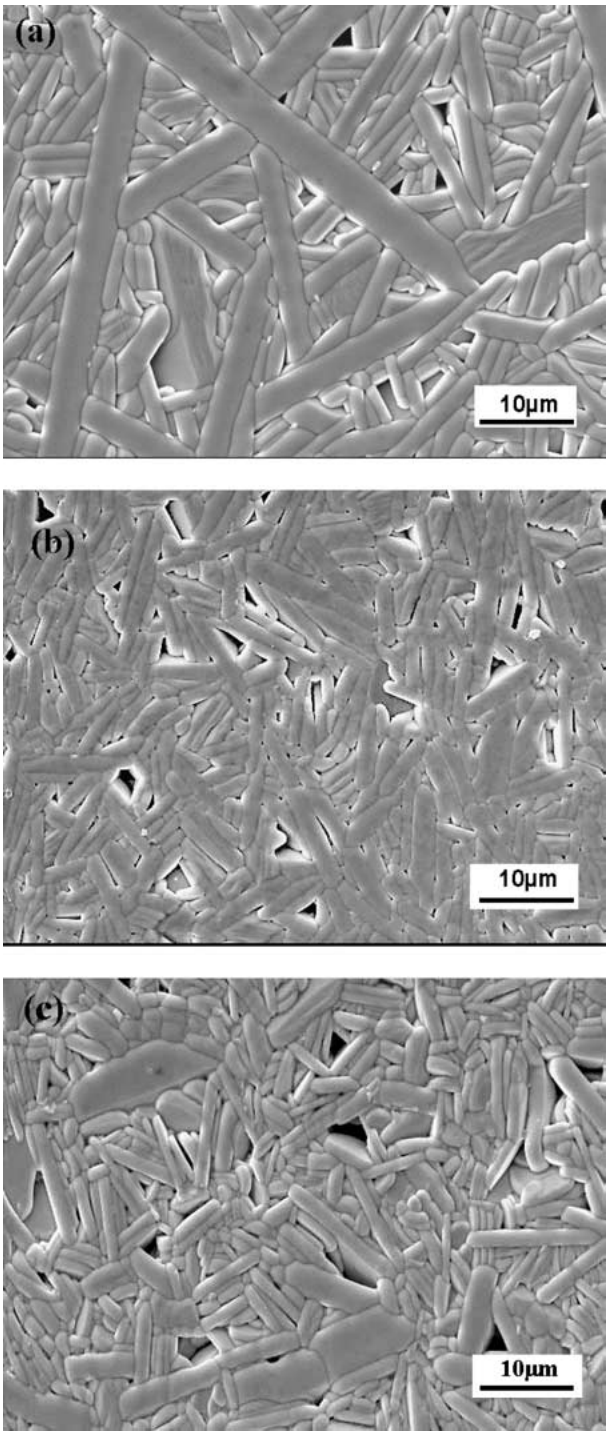

Figure 3 Scanning electron micrographs of polished and etched sections of (a) nominal $Bi_4Ti_3O_{12}$, (b) Bi_2O_3-rich $Bi_4Ti_3O_{12}$, and (c) TiO_2-rich $Bi_4Ti_3O_{12}$ after sintering for 1 h at 1100°C.

Fig. 3 shows that the microstructures of nominally stoichiometric $Bi_4Ti_3O_{12}$, Bi_2O_3-rich $Bi_4Ti_3O_{12}$, and TiO_2-rich $Bi_4Ti_3O_{12}$ after sintering for 1 h at 1100°C. The three microstructures show a random arrangement of elongated grains and the Lotgering factors for all three samples are in the range of 0.2–0.3. Several highly elongated grains are seen in the microstructure for the nominal $Bi_4Ti_3O_{12}$ composition (Fig. 3a) but not in the microstructures for the Bi_2O_3-rich $Bi_4Ti_3O_{12}$ composition (Fig. 3b) and the TiO_2-rich $Bi_4Ti_3O_{12}$ composition (Fig. 3c). The differences in the grain size

and the grain aspect ratio may be related to the sintering onset temperature, which is dependent on the composition.

It is commonly observed that densification during sintering is hindered by the concurrent growth of randomly aligned, highly elongated grains, particularly when significant elongated grain growth occurs in the earlier stages of sintering [27]. High final densities are difficult to achieve because matter transport into the interstices between highly elongated grains is normally difficult by solid state diffusion. In the present system, microstructural observations (not reported here) of samples sintered to relative densities in the range of 0.80–0.95 indicate that the highly elongated grains start to develop after significant densification has been achieved (when the relative density is greater than ∼0.90). The effect of the elongated grains in hindering densification in the present system is therefore limited.

Hot forging experiments on nominal $Bi_4Ti_3O_{12}$ powder compacts indicated that both the fabrication temperature and the initial density of the body are key variables in optimizing the grain alignment. Low fabrication temperatures produced inadequate densification and reduced grain alignment. Low initial density (60–70% of the theoretical) of the hot forged materials required long times to achieve adequate densification and grain alignment while high initial densities (>90%) resulted in some degree of cracking during sinter forging. A temperature of ∼1050°C and intermediate initial densities (relative densities of 80–85%) produced dense microstructures with highly aligned grains.

Fig. 4 shows data for the axial strain rate of the nominally stoichiometric $Bi_4Ti_3O_{12}$ powder compacts (initial relative density ≈0.80) as a function of time at four hot forging temperatures and under a uniaxial stress of 5 MPa. A rapid increase in the strain rate at early times is observed above 870°C, a temperature that corresponds to the onset of sintering in this system. For $Bi_4Ti_3O_{12}$ with an initial density of 0.80 prepared by sintering (Lotgering factor = 0.2–0.3), Fig. 5 shows the data for the density and Lotgering factor as a function of hot forging time at 1050°C. In the experiments, the pressure was applied when the isothermal sintering

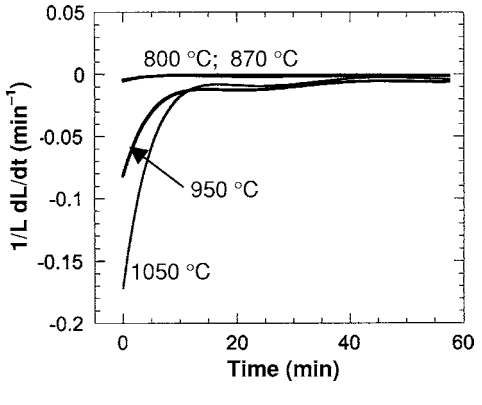

Figure 4 Axial strain rate versus time for nominal $Bi_4Ti_3O_{12}$ powder compacts hot forged under a constant stress of 5 MPa at different temperatures.

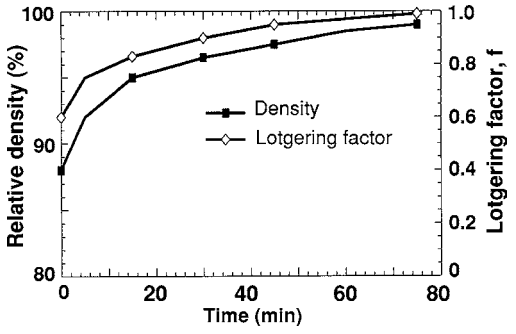

Figure 5 Variation of density and Lotgering factor for nominal $Bi_4Ti_3O_{12}$ powder compacts (initial density = 0.80 of the theoretical) as a function of hot forging time at 1050°C and under a pressure of 5 MPa.

temperature was reached, and zero time was taken as the time when the pressure reached the required value of 5 MPa. The data show a rapid increase in the Lotgering factor and in the density as the pressure was being applied and during the early stages of hot forging. These data, coupled with the data of Fig. 4, indicate that a rearrangement process may be playing a key role in the early stages of hot forging. As the rearrangement process slows, diffusional mass transport is expected to become important.

Scanning electron micrographs of surfaces perpendicular and parallel to the hot forging direction are shown in Fig. 6 for the nominally stoichiometric

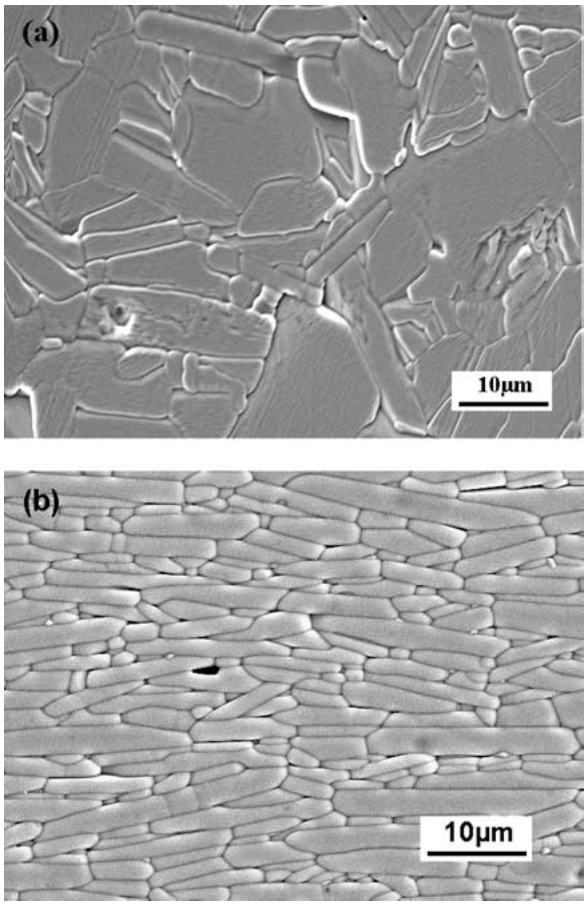

Figure 6 Scanning electron micrographs of nominal $Bi_4Ti_3O_{12}$ powder compact hot forged for 75 min at 1050°C under a pressure of 5 MPa showing planes: (a) perpendicular and (b) parallel to the hot forging direction.

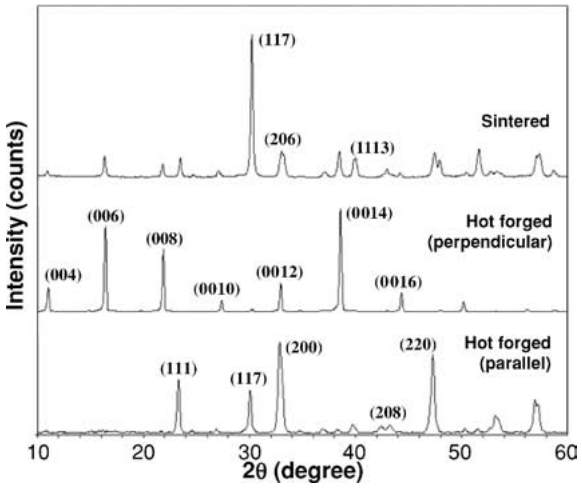

Figure 7 X-ray diffraction patterns of nominal $Bi_4Ti_3O_{12}$ powder compacts sintered for 1 h at 1100°C and hot forged for 75 min at 1050°C showing texture development in planes parallel and perpendicular to the hot forging direction.

$Bi_4Ti_3O_{12}$ composition hot forged for 75 min at 1050°C under a uniaxial stress of 5 MPa. The final relative density of the sample was ∼0.98 and the Lotgering factor was ∼0.97. The grains show good alignment perpendicular to the hot forging direction (Fig. 6b) whereas the surface perpendicular to the hot forging direction (Fig. 6a), with the large areal dimensions compared to the thickness, indicates that the grains have a plate-like shape.

Fig. 7 shows a comparison of X-ray diffraction patterns for the sintered $Bi_4Ti_3O_{12}$ powder compacts (1 h at 1100°C) with a random arrangement of the grains and for the hot forged $Bi_4Ti_3O_{12}$ (75 min at 1050°C) for surfaces perpendicular and parallel to the hot forging direction. Diffraction from the (00*l*) planes in the surface perpendicular to the hot forging direction indicates that the grains are oriented along the *c*-axis.

The influence of compositional variation on the axial strain rate during hot forging is shown in Fig. 8 for the nominally stoichiometric $Bi_4Ti_3O_{12}$, Bi_2O_3-rich $Bi_4Ti_3O_{12}$, and TiO_2-rich $Bi_4Ti_3O_{12}$ compositions. At the equivalent temperature, the Bi_2O_3-rich composition

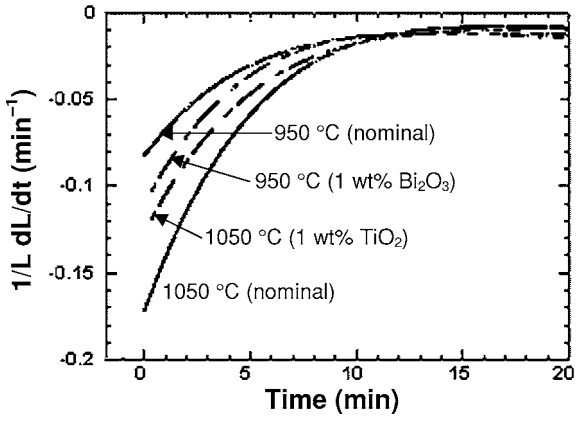

Figure 8 Axial strain rate versus time for nominal $Bi_4Ti_3O_{12}$, Bi_2O_3-rich $Bi_4Ti_3O_{12}$, TiO_2-rich $Bi_4Ti_3O_{12}$ compacts hot forged under a constant stress of 5 MPa.

deforms more readily whereas the TiO_2-rich composition deforms more slowly than the nominally stoichiometric composition. These trends in the hot forging kinetics follow those described earlier for the sintering kinetics.

Compositional effects on the hot forged microstructure are shown in Fig. 9. For Bi_2O_3-rich $Bi_4Ti_3O_{12}$, Fig. 9a shows a scanning electron micrograph of the material hot forged for 75 min at 950°C. The microstructure shows significant grain alignment and the presence of nearly equiaxial second phase grains identified to be $Bi_{12}TiO_{20}$ by X-ray diffraction. It is believed that the second phase grains developed by the crystallization of a liquid phase when the material was cooled to room temperature. Corresponding micrographs for the nominal $Bi_4Ti_3O_{12}$ and for TiO_2-rich $Bi_4Ti_3O_{12}$ (1 wt% excess TiO_2) hot forged for 75 min at 1050°C are shown in Fig. 9b and c. Both materials show considerable grain alignment. In addition, the TiO_2-rich $Bi_4Ti_3O_{12}$ contains a dispersed second phase of fine particles identified to be $Bi_2Ti_4O_{11}$ by XRD. For the TiO_2-rich $Bi_4Ti_3O_{12}$, the presence of the $Bi_2Ti_4O_{11}$ phase is in agreement with phase diagram data and the formation of a liquid phase is not expected until the temperature reaches ∼1210°C [19], a value that is considerably higher than that used in the experiment (1050°C).

According to Fig. 9a–c, considerable grain alignment is achieved regardless of the presence of a solid or liquid second phase. The data indicate that a liquid phase may facilitate the achievement of significant grain orientation but it is not a requirement. Lotgering factors for the sintered materials (see Fig. 3) and the hot forged materials (see Fig. 9a–c) are summarized in Table I.

Fig. 9d–f show scanning electron micrographs of the hot forged materials after they were annealed in air for 2 h at 1100°C. For the Bi_2O_3-rich $Bi_4Ti_3O_{12}$, (Fig. 9d), the most significant change is the development of large angular pores, which may be caused by the evaporation of the Bi_2O_3-rich second phase (liquid at the annealing temperature) or by removal of some grains during the sample preparation (e.g., grinding and polishing). The removal of the second phase is supported by X-ray diffraction data which show that the annealed material consists of single phase $Bi_4Ti_3O_{12}$. The annealed TiO_2-rich sample (Fig. 9f) also retained the grain alignment of the hot forged material but the presence of very fine pores, presumably caused by the disappearance of the $Bi_2Ti_4O_{11}$ particles, is observed. The most drastic microstructural change during annealing is found for the nominal $Bi_4Ti_3O_{12}$ composition (Fig. 9e) where

TABLE I Lotgering factors of the sintered and hot forged $Bi_4Ti_3O_{12}$ materials

Composition	Sintered[a]	Hot forged
$Bi_4Ti_3O_{12}$ + 1 wt% Bi_2O_3	0.2–0.3	0.90[b]
$Bi_4Ti_3O_{12}$	0.2–0.3	0.97[c]
$Bi_4Ti_3O_{12}$ + 1 wt% TiO_2	0.2–0.3	0.95[c]

[a]1 h at 1100°C.
[b]75 min at 950°C and 5 MPa.
[c]75 min at 1050°C and 5 MPa.

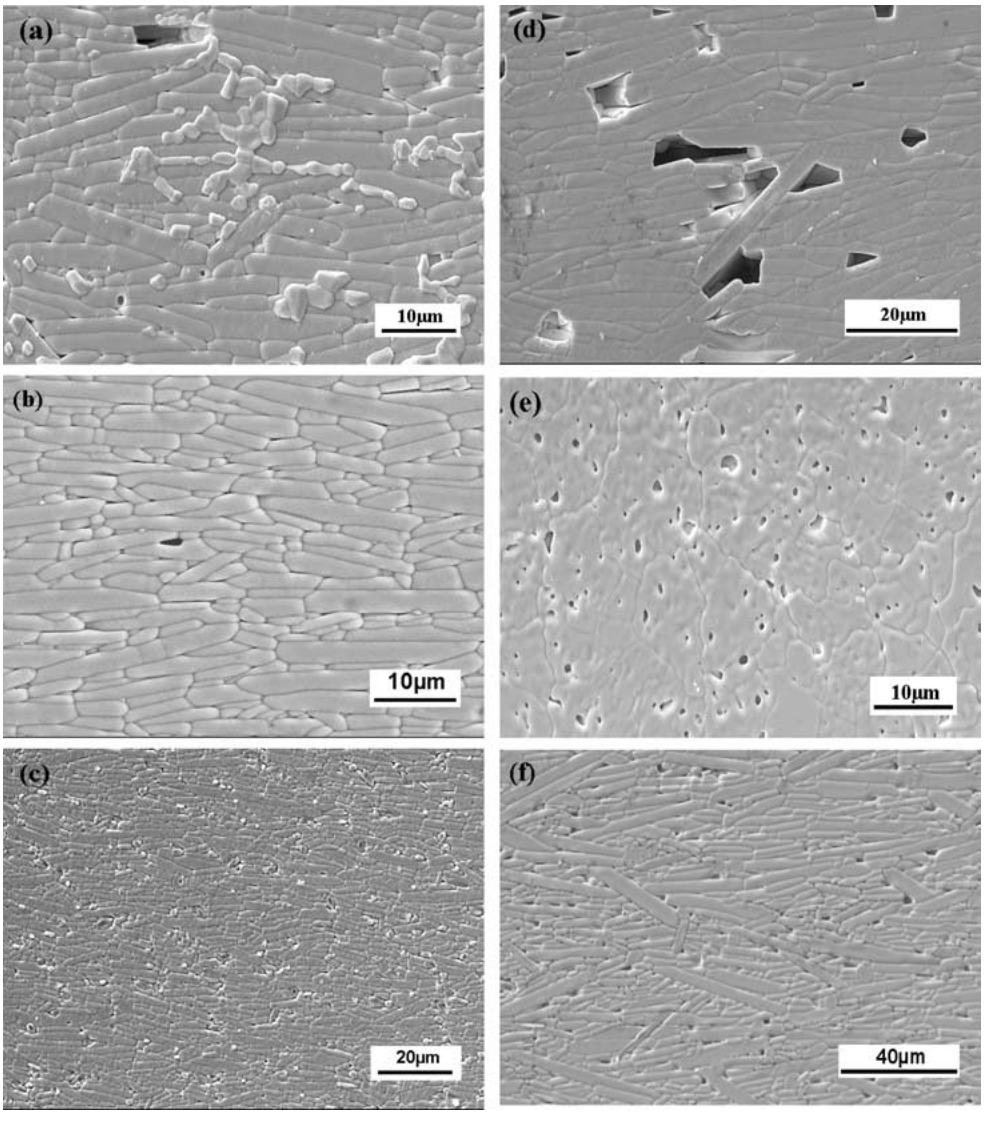

Figure 9 Scanning electron micrographs showing the effect of small compositional variations on the hot-forged microstructure (a)–(c). The effect of annealing for 2 h at 1100°C on the hot forged microstructure is shown in (d)–(f). The sample compositions are Bi_2O_3-rich $Bi_4Ti_3O_{12}$ (a), (d); nominal $Bi_4Ti_3O_{12}$ (b), (e); and TiO_2-rich $Bi_4Ti_3O_{12}$ (c), (f).

the grain alignment has completely disappeared. The grain boundaries are irregular and the microstructure also shows evidence of de-sintering, as seen from the presence of a significant amount of porosity. It is not clear why the aligned grain microstructure of the hot forged, nominal $Bi_4Ti_3O_{12}$ composition is destroyed so remarkably during subsequent annealing. Further work is being carried out to understand the microstructural changes.

4. Conclusions

Nearly fully dense $Bi_4Ti_3O_{12}$ (relative density ≈0.98) with significant grain alignment (Lotgering factor ≈0.97) was produced by hot forging of powder compacts with a sintered density of 80–85% of the theoretical value under moderate pressures (∼5 MPa) and at temperatures in the range of 950–1050°C. Compositional variations (from TiO_2-rich to Bi_2O_3-rich $Bi_4Ti_3O_{12}$) coupled with phase diagram data indicate that a liquid phase can facilitate the achievement of grain orientation but it is not a requirement. Significant grain alignment can be achieved with or without the presence or a liquid phase during hot forging. Microstructural evolution of hot forged $Bi_4Ti_3O_{12}$ during subsequent annealing in air at 1100°C is highly dependent on the composition. For the nominal $Bi_4Ti_3O_{12}$ composition, the grain alignment was completely disrupted and some de-sintering occurred. The TiO_2-rich and Bi_2O_3-rich compositions retained the grain alignment but developed a small amount of porosity presumably caused by the removal of second phases.

References

1. J. RODEL and A. M. GLAESER, *J. Amer. Ceram. Soc.* **73** (1990) 3292.
2. M. SEABAUGH, D. HORN, I. KERSCHT, S.-H. HONG and G. L. MESSING, in "Sintering Technology," edited by R. M. German, G. L. Messing and R. G. Cornwall (Marcel Dekker, New York, 1996) p. 341.
3. S.-H. HONG and G. L. MESSING, *J. Amer. Ceram. Soc.* **81** (1998) 1269.
4. T. S. HUANG, M. N. RAHAMAN, T.-I. MAH and T. A. PARTHASARATHAY, *ibid.* **83** (2000) 204.
5. H. S. SHULMAN, M. TESTORF, D. DAMJANOVIC and N. SETTER, *ibid.* **79** (1996) 3124.

6. U. KUNAVER and D. KOLAR, *Acta Metall. Mater.* **41** (1993) 2255.
7. J. U. KNICKERBOCKER and D. A. PAYNE, *Ferroelectrics* **37** (1981) 733.
8. T. TAKENAKA and K. SAKATA, *Jpn. J. Appl. Phys.* **19** (1980) 31.
9. T. KIMURA, T. YOSHIMOTO, N. IIDA, Y. FUJITA and T. YAMAGUCHI, *J. Amer. Ceram. Soc.* **72** (1989) 85.
10. Y. INOUE, T. KIMURA, T. YAMAGUCHI, K. NAGATA and K. OKAZAKI, *Jpn. J. Appl. Phys.* **20** (1983) 95.
11. S. SWARTZ, W. A. SCHULZE and J. V. BIGGERS, *Ferroelectrics* **38** (1981) 765.
12. H. WATANABE, T. KIMURA and T. YAMAGUCHI, *J. Amer. Ceram. Soc.* **72** (1989) 289.
13. J. A. HORN, S. C. ZHANG, U. SELVARAJ, G. L. MESSING and S. TROILER-MCKINSTRY, *ibid.* **82** (1999) 921.
14. S.-H. HONG, S. TROLIER-MCKINSTRY and G. L. MESSING, *ibid.* **83** (2000) 113.
15. A. FOUSKOVA and L. E. CROSS, *J. Appl. Phys.* **41** (1970) 2834.
16. S. E. CUMMINS and L. E. CROSS, *Appl. Phys. Lett.* **10** (1967) 14.
17. *Idem.*, *J. Appl. Phys.* **39** (1968) 2268.
18. Y. MASUDA, H. MASUMOTO, A. BABA, T. GOTO and T. HIRAI, *Jpn. J. Appl. Phys.* **31** (1992) 3108.
19. E. I. SPERANSKAYA, I. S. REZ, L. V. KOZLOVA, V. M. SKORILOV and V. I. SLAVOV, *Izv. Akad. Nauk. SSSR, Neorg. Mater.* **1** (1965) 232.
20. T. M. BRUTON, *J. Solid State Chem.* **9** (1974) 173.
21. E. M. LEVIN and R. S. ROTH, *J. Res. Nat. Bur. Stds.* A **68** (1964) 197.
22. A. D. MORRISON, *Ferroelectrics* **2** (1971) 59.
23. J. F. DORRIAN, R. E. NEWNHAM, D. K. SMITH and M. I. KAY, *ibid.* **3** (1971) 17.
24. F. K. LOTGERING, *J. Inorg. Nucl. Chem.* **9** (1959) 113.
25. M. N. RAHAMAN, L. C. DE JONGHE, J. A. VOIGT and B. A. TUTTLE, *J. Mater. Sci.* **25** (1990) 737.
26. J. LUO, H. WANG and Y.-M. CHIANG, *J. Amer. Ceram. Soc.* **82** (1999) 916.
27. M. N. RAHAMAN, "Ceramic Processing and Sintering," 2nd ed. (Marcel Dekker, New York, 2003).

Received 4 March
and accepted 19 August 2003